PERGAMON

International Journal of Solids and Structures 40 (2003) 5389–5406

INTERNATIONAL JOURNAL OF SOLIDS and STRUCTURES

www.elsevier.com/locate/ijsolstr

Crack parameter estimation in structures using finite element modeling

Mohammad H.F. Dado [a], Omar A. Shpli [b,*]

[a] Department of Mechanical Engineering, Faculty of Engineering and Technology, University of Jordan, Jordan
[b] Department of Mechanical Engineering, Faculty of Engineering, Hashemite University, Al-zarqa 13115, Jordan

Received 16 October 2002; received in revised form 16 April 2003

Abstract

This paper addresses the problem of linear crack quantification, crack depth estimation and localization, in structures. An optimization technique based on a finite element model for cracked structural elements is employed in the estimation of crack parameters for beam, truss and two-dimensional frame structures. The modal data for the cracked structures are obtained by solving the corresponding eigenvalue problem. The error in the modal data is simulated by an additive noise that follows the normal distribution. The simulated reduced modal data is expanded using the eigenvector projection method. Numerical examples showed that this technique gives good results for cracks with high depth ratio. The accuracy of the estimated crack parameters depends on (1) the number of modes used, (2) the error level in the cracked structure modal data and (3) the number of measured degrees of freedom in the case of reduced modal data.

Keywords: Fault detection; Health monitoring; Crack parameter estimation; Finite element modeling; Cracked structures; Beam; Trusses; Two-dimensional frames

1. Introduction

In the past few years the problem of health monitoring and fault detection of structures has received considerable consideration. It was noted that fault cause changes in the dynamic response of the structure. The changes can be considered as an indication of the health of the structure. Consequently, these methods of fault detection are based on the comparison of the dynamic response of the healthy structure with the dynamic response of the defected structure.

The comparison is carried out through some algorithm, which employs the modal data of the healthy and defected structure. Therefore, the fault detection problem is dependant on the modal data for the healthy structure, the modal data for the defected structure and the algorithm that uses these data and

* Corresponding author.
E-mail address: omaralshibli@yahoo.com (O.A. Shpli).

0020-7683/$ - see front matter © 2003 Elsevier Ltd. All rights reserved.
doi:10.1016/S0020-7683(03)00286-5

provides information about the state of the structure. Each of these items has its own aspects and associated problems that affect the results of the fault detection.

In fault detection literature, four different levels for fault detection have been identified. The first level is the detection of a fault in which the algorithm just indicates that a fault exists in the structure. This level is the simplest level and a simple comparison of the modal data for the healthy and defected structures can achieve this task. In level two, the algorithm locates the defect in the structure. Level three in fault detection gives an estimate of the severity of the defect in addition to the detection and localization (levels one and two). The last level (level four) is that which provides an estimate of the remaining operational life of the structure.

Several algorithms for fault detection were invented and developed during the past few years. The differences between these algorithms are the type of dynamic data that is used and the level of detection. A full literature survey for the fault detection and health monitoring of structures, is presented by Scott et al. (1996) and Mottershead and Friswell (1993). The methods that are based on the frequency change are classified as either forward (Fox, 1992; Friswell et al., 1994) or inverse problems (Dado, 1997; Dado and Abuzid, in press). Such methods have a significant limitation because of the low sensitivity of the natural frequencies for cracks with small depth. Therefore, high level of defect or measurements with high accuracy is required for the detection of cracks with small depth. These methods are considered as level one (detection).

The second set of algorithms is based on the change in mode shapes. The modal assurance criteria (MAC) as an indication about the location of a defect, was first introduced by West (1984). Since then several different measures for the fault detection such as the partial modal assurance (PMAC) and coordinate modal assurance (COMAC) criterion (Kim and Bartkowicz, 1993) and the structural translational and rotational error check (Mays, 1992), were developed. These algorithms do not need a model for the defected structure, which is considered as being their main advantage. A similar set of algorithms uses the change in the mode shape curvature or the strain mode shapes as an alternative for the mode shapes. These methods have the same advantage that is they do not need a model for the structure.

Another class of fault detection algorithms are based on the dynamically measured flexibility matrix of the defected structure, similar to these methods that are based on the change on mode shapes, different criterion were developed to provide and indication about the defect. The direct comparisons of the flexibility of the heathery and delectated structure (Pandy et al., 1991), the unity check method (Lin, 1990) and the stiffness error matrix (Park et al., 1988) were used throughout the fault detection literature.

Matrix update methods (Simth, 1992; Linder and Goff, 1993; Kaouk and Zimmerman, 1994) are based on modifying the structure matrices (mass, stiffness and damping matrices) such that the modal data for the defected structure is reproduced. The differences between these methods are the objective function, the constraints definition and the numerical schemes employed in the optimization.

In such a method, a model for the healthy and defected structures is required. The finite element method is usually used in modeling of the healthy and defected structures. It is usually assumed that the defect affects the stiffness matrix of the defected element but not the mass matrix. The stiffness matrix is represented as a certain fraction of the healthy element stiffness matrix (Abdalla et al., 2000; Kaouk and Zimmerman, 1994) or a localized reduction in the modulus of elasticity. This method is considered as a level three fault detection method.

Many other researches have addressed different issues in fault detection like the effect of noise in the measured modal data, the number of modes used in fault detection, using reduced modal data and applying different schemes in the optimization (Abdalla et al., 2000; Kaouk et al., 1994; Friswell et al., 1997, 1998). It is noted that the fault detection algorithms generally localize the defect by identifying the defected element and the fault severity is indicated as a reduction in the element stiffness. The fourth level of fault detection that provides an estimate of the remaining operational life, needs more information about the defect parameters and the information provided by these fault detection algorithms are not sufficient. Naturally,

acquiring more specific information about the defect, which can be used in the fourth level of fault detection, needs a model for the defect that relates the defect parameters to the change in structure dynamic properties (mass, stiffness and damping matrices). Such a model, if available, can be employed in fault detection.

Structures are generally subjected to different forms of faults such as failure of joints, cracks and buckling or complete loss of elements. These defects are generally nonlinear and difficult to model, which can be considered as the main reason for trying to develop fault detection algorithms that do not need a model for the fault such as MAC and the PMAC. However, cracks are the most common type of defects that occur in structures. Much has been done to model the effect of cracks in simple structural elements such as axially loaded members and beams. It was found that analytical modeling of cracks is very difficult especially for practical structures with multiple cracks.

Shpli and Dado (submitted for publication) described a procedure for derivation of modeling finite structural elements with linear (open) cracks in terms of the crack parameters. They derived stiffness matrices for rode, beam and two-dimensional frame finite elements. The derived models are function in the crack depth ratio and the crack location (crack parameters). These models were used in estimating the natural frequencies for beam, truss and two-dimensional frame structures and verified by comparing their results with published experimental and analytical data.

This study employs these models in crack parameter estimation for structures that contain defected elements. The effect of the noise in the modal data, number of modes used and using reduced modal data will be studied for beam, three-dimensional trusses and two-dimensional frame structures. The modal data for the defected structures are obtained by solving the corresponding eigenvalue problem for the cracked structures and the noise is simulated by an additive white noise.

2. Cracked structure model

A crack, when presented in a structural element causes a reduction in the stiffness matrix of the element. Therefore, the stiffness matrix of a cracked element is expected to be a function of the crack depth and the crack location. Shpli and Dado (submitted for publication) have presented a general procedure for modeling cracked finite structural element. In their model the crack was represented by a localized compliance and the stiffness matrix of the cracked element is expressed in terms of the crack compliance and location in addition to the material and geometrical properties. In general the cracked element stiffness matrix is given by

$$\mathbf{K}_{\mathrm{d}} = \mathbf{K}_{\mathrm{d}}(c, x) \tag{1}$$

where $\mathbf{K}_{\mathrm{d}}$ is the cracked element stiffness matrix, c is the crack compliance and x is the crack location in elemental local coordinates. This stiffness matrix can be used to model healthy as well as cracked elements because it is reduced to the healthy element stiffness matrix when the crack compliance is zero.

The localized stiffness for a cracked element is function of the crack depth, type of loading, and mode of deformation in addition to the geometrical and material properties of the element. The localized stiffness of a crack is given by (Dimarogonas and Stephen, 1983):

$$c_{ij} = \frac{\partial u_i}{\partial P_j} = \frac{\partial}{\partial P_j \partial P_i} \int_0^a J(\zeta)\,\mathrm{d}\xi \tag{2}$$

where $J(a)$ is the strain energy density function, P_j is the force that causes the deformation, P_i is the force in the direction of deformation and a is the crack depth. The strain energy density function is given by

$$J(a) = \frac{1}{E'} \int_0^B \left(\left(\sum_{i=1}^{6} K_{\mathrm{I}i} \right)^2 + \left(\sum_{i=1}^{6} K_{\mathrm{II}i} \right)^2 + \alpha \left(\sum_{i=1}^{6} K_{\mathrm{III}i} \right)^2 \right) \mathrm{d}\zeta \tag{3}$$

where K is the stress intensity factor for the crack in different modes of deformation, which is a function of the crack depth, B is the width of the element cross-section, E is the modulus of Elasticity, v is the Poisson's ratio, E' is E for plane stress and $E/(1-v)$ for plane strain and $\alpha = 1 + v$. Substituting Eq. (3) in the Eq. (2) gives the general equation for the crack compliance, which is given by

$$c_{ij} = \frac{1}{E'} \frac{\partial^2}{\partial P_j \partial P_i} \int_0^B \int_0^a \left(\left(\sum_{i=1}^{6} K_{\mathrm{I}i} \right)^2 + \left(\sum_{i=1}^{6} K_{\mathrm{II}i} \right)^2 + \alpha \left(\sum_{i=1}^{6} K_{\mathrm{III}i} \right)^2 \right) \mathrm{d}\xi \, \mathrm{d}\zeta \tag{4}$$

In general, a crack is subjected to six different types of loading three forces and three moments along the x, y and z directions. Therefore, the crack compliance has 36 components, which are arranged in a 6×6 matrix. This matrix is symmetric because of the reciprocity property of the compliance.

Shpli and Dado (submitted for publication) derived a cracked stiffness matrix for truss, beam and two-dimensional frame elements. These models are presented in Appendix A Eqs. (A.1)–(A.3). These equations were derived by considering a cracked finite element that has a crack depth a and located at x form the start node of the finite element. The cracked element was modeled as two healthy finite elements that are coupled by a localized compliance element, which represents the effect of the crack. The nodal displacements nodal forces relations for the overall element were derived and re-arranged in the finite element form.

The derived models were used to predict the vibration response of several types of engineering structures with multiple cracks. These models were verified by comparing the vibration response of different types of engineering structures that have cracked elements with published experimental and theoretical results. The comparison has indicated an excellent agreement between the results obtained by employing these models and the published results.

These models that are presented in Eqs. (A.1)–(A.3) are function of the crack compliance and crack location in addition to the element material and geometrical properties. In addition, these models are reduced to the stiffness matrices of healthy finite elements if the crack compliance is zero. If the crack compliance approaches infinity, which corresponds to a completely failed element, the stiffness matrices are reduced to the zero matrices.

If these finite element models are used in modeling of a cracked structure, the global stiffness matrix of the structure can be written as a function of the crack depth and crack location in addition to the geometrical and material properties of the element. i.e.:

$$K = K(\boldsymbol{a}, \boldsymbol{x}) \tag{5}$$

where $\boldsymbol{a}$ and $\boldsymbol{x}$ are the vectors of crack depth and crack location in element local coordinate system.

3. Crack parameter estimation

3.1. Objective function

The crack parameter estimation is the process of finding the set of crack parameters (crack depth and crack location) that reproduce the modal data (natural frequencies and mode shapes) of the defected structure. Many objective functions have been suggested to formulate this problem. One objective function (Ruotolo and Surace, 1997) is based on minimizing the difference between the measured and estimated modal data. Mathematically this objective function is given by

$$\text{minimize} \sum_i \|\omega_{i\mathrm{d}} - \omega_{i\mathrm{h}}\| + \|U_{i\mathrm{d}} - U_{i\mathrm{h}}\| \tag{6}$$

where $U_{i\mathrm{d}}$ and $U_{i\mathrm{h}}$ are the ith mode defected and healthy mode shapes. $\omega_{i\mathrm{d}}$ and $\omega_{i\mathrm{h}}$ are the ith natural frequencies for the healthy and defected structures.

A different form (Abdalla et al., 2000), which is used in this study, is based on finding the crack parameters vector that minimizes the difference between the healthy and defected stiffness matrices, and at the same time satisfy the eigenvalue equation and the corresponding constrains on the crack location and crack depth ratio. In this form the modal data of the cracked structure is used as a constraint. Using this objective function the problem can be stated as follows.

Given the modal data for the first m modes of a structure that consists of n elements, it is required to find the crack location x_i and the crack depth ratio $(a/w)_i$ $(i = 1, 2, \ldots, n)$ that minimizes the Frobenius norm of the difference between the healthy and defected stiffness matrices i.e.:

$$\text{minimize} \|K_{\mathrm{h}} - K_{\mathrm{d}}((a/w)_i, x_i)\| \tag{7}$$

Subjected to the constraints:

$$0 \leqslant x_i \leqslant l_i \tag{8}$$

$$0 \leqslant (a/w)_i \leqslant 1 \tag{9}$$

$$\|K_{\mathrm{d}} u_j - \omega_j^2 M u_j\| = 0 \quad i = 1, 2, \ldots, n \quad \text{and} \quad j = 1, 2, \ldots, m \tag{10}$$

where K_{d} is the stiffness matrix for the defected structure, K_{h} is the stiffness matrix for the healthy structure, M is the mass matrix of the structure, u_j is the jth measured mode shape for the defected structure, ω_j is the natural frequency corresponding to the jth mode shape of the defected structure, n is the number of elements in the structure and m is the number of modes of the defected structure that are used in the crack parameter estimation.

In certain cases of defected structures, a set of distributed cracks within the structures may produce the same mode-shapes as that of the actual state of defect. However, the natural frequencies will not be the same definitely, in the sense that both the mode-shapes and natural frequencies are being involved in the modal-data constraint, i.e., Eq. (10). Thus the optimization problem will converge to the actual state of defect. In addition, in case of structures that having symmetrical conditions of geometry, material and boundary conditions, two different states of defect in two symmetrical elements can produce the same natural frequencies. On the other hand, the mode-shapes will be different which ensures that the optimization algorithm will converge to the actual state of defect due to the same reason.

The first two constraints that are presented in Eqs. (8) and (9) are classified as geometrical constraints while the third constraint, Eq. (10), is known as natural constraint. The eigenvalue constraint given by Eq. (10) can not be satisfied exactly because of the errors in the experimental modal data and round off errors. Therefore, it is always replaced by

$$\|K_{\mathrm{d}} u_j - \omega_j^2 M u_j\| \leqslant \varepsilon \tag{11}$$

where ε is the eigenvalue constraint tolerance. The value of this tolerance depends on the error in the modal data and the required accuracy in the estimated crack parameters. This parameter is given an initial value and then reduced successively. Each time, the problem is solved with the new value of ε and the norm of the resulting solution vector is compared with the norm of the solution vector for the previous value of ε, this process is continued untill the change in the norm of the solution vector with the reduction of ε is negligible.

This set of constraints along with the objective function forms a convex programming problem. Hence, any optimization solution procedure will converge to the global minimum. Each constraint in Eqs. (8) and (9) actually, represents two constraints. Writing the constraints in the standard form one gets:

$$g_{1i} = -x_i \leqslant 0 \tag{12}$$

$$g_{2i} = x_i - l_i \leqslant 0 \tag{13}$$

$$g_{3i} = -(a/w)_i \leqslant 0 \tag{14}$$

$$g_{4i} = (a/w)_i - 1 \leqslant 0 \tag{15}$$

$$g_{5j} = \|K_d u_j - \omega_j^2 M u_j\| - \varepsilon \leqslant 0 \quad i = 1, 2, \ldots, n \quad \text{and} \quad j = 1, 2, \ldots, m \tag{16}$$

This problem can be transformed into unconstrained optimization problem using the exterior penalty functions. This is an appropriate choice since the resulting objective function is continuous and there is no constraints on the initial guess. Using external penalty functions the objective function becomes:

$$F = \|\mathbf{K}_h - \mathbf{K}_d(x_i, (a/w)_i)\| + r\sum_{i=1}^{n}\left(\langle g_{1i}\rangle^2 + \langle g_{2i}\rangle^2 + \langle g_{3i}\rangle^2 + \langle g_{4i}\rangle^2\right) + r\sum_{j=1}^{m}\langle g_{5j}\rangle^2 \tag{17}$$

$$\langle g_{ki}\rangle = \begin{cases} g_{k1i} & g_{ki} > 0 \\ 0 & g_{ki} \leqslant 0 \end{cases}$$

$$\langle g_{5i}\rangle = \begin{cases} g_{5i} & g_{5i} > 0 \\ 0 & g_{5i} \leqslant 0 \end{cases}$$

$$k = 1, 2, 3, 4, \ i = 1, 2, \ldots, n \ \text{and} \ j = 1, 2, \ldots, m$$

The optimum solution for this optimization problem can be found using any search method for solving optimization problems, such as the univariate or the steepest descent direction with optimal step length.

3.2. Reduced modal data

In practical fault detection problems the number of degrees of freedom is usually very large. In addition some of the degrees of freedom are difficult or cannot be measured. Therefore the number of degrees of freedom that are used in the fault detection is usually less than the total number of degrees of freedom in the structure. This affects directly the modal data constrain, which is given by

$$[\mathbf{K}_d - \omega_j^2 \mathbf{M}]\mathbf{u} = [0] \tag{18}$$

This constraint, which has the general form:

$$\mathbf{B}\mathbf{u} = \mathbf{0} \tag{19}$$

uses all the degrees of freedom in the structure (measured or unmeasured). It must either be replaced by an equation that contains only the measured degrees of freedom (matrix reduction) or the eigenvector u must be expanded by estimating the unmeasured degrees of freedom. Many schemes can be used to perform this task. The simplest one is that known as Guyan reduction. In the scheme Eq. (19) can be written in the form of two matrix equations such that:

$$\mathbf{B}_{11}\mathbf{u}_k + \mathbf{B}_{12}\mathbf{u}_u = \mathbf{0} \tag{20}$$

$$\mathbf{B}_{21}\mathbf{u}_k + \mathbf{B}_{22}\mathbf{u}_u = \mathbf{0} \tag{21}$$

where $\mathbf{u}_k$ is the vector of known eigenvalues, $\mathbf{u}_u$ is the vector of unknown eigenvalues and $\mathbf{B}_{ij}$ are sub matrices obtained by partitioning the matrix $\mathbf{B}$. Eq. (21) can be solved for the unknown vector of eigenvalues, which gives

$$\mathbf{u}_u = -\mathbf{B}_{22}^{-1}\mathbf{B}_{21}\mathbf{u}_k \tag{22}$$

and the expanded eigenvector is given by

$$\mathbf{u} = \begin{bmatrix} \mathbf{I} \\ -\mathbf{B}_{22}^{-1}\mathbf{B}_{21} \end{bmatrix} \mathbf{u}_k \tag{23}$$

substituting Eq. (23) into Eq. (20) yields the reduced eigenvalue constraint equation, which is given by

$$[\mathbf{B}_{11} - \mathbf{B}_{12}\mathbf{B}_{22}^{-1}\mathbf{B}_{21}]\mathbf{u}_k = 0 \tag{24}$$

This equation can be used instead of the eigenvalue constraint Eq. (20).

Another scheme (Friswell et al., 1998), which is known as the mode shape projection algorithm, is based on finding the vector of unknown eigenvalues that minimizes the error force vector. In fault detection literature, the error force vector R is given by

$$R = -[\mathbf{K} - \omega_i^2\mathbf{M}] \begin{bmatrix} \mathbf{u}_k \\ \mathbf{u}_\mathrm{u} \end{bmatrix} = [\, \mathbf{Z}_1 \quad \mathbf{Z}_2 \,] \begin{bmatrix} \mathbf{u}_k \\ \mathbf{u}_\mathrm{u} \end{bmatrix} \tag{25}$$

The vector of unknown eigenvalues is the one that minimizes the norm of R i.e.:

$$\mathbf{u}_\mathrm{u} = \min_{\mathbf{u}_\mathrm{u}} (R^T R) \tag{26}$$

which has the minimizing solution:

$$\mathbf{u}_\mathrm{u} = -(\mathbf{Z}_2^T\mathbf{Z}_2)^{-1}\mathbf{Z}_2^T\mathbf{Z}_1\mathbf{u}_k \tag{27}$$

the expanded eigenvector becomes:

$$\mathbf{u} = \begin{bmatrix} I \\ -(\mathbf{Z}_2^T\mathbf{Z}_2)^{-1}\mathbf{Z}_2^T\mathbf{Z}_1 \end{bmatrix} \mathbf{u}_k \tag{28}$$

the reduced eigenvalue constraints equation becomes:

$$\begin{bmatrix} \mathbf{B}_{11} - \mathbf{B}_{12}(\mathbf{Z}_2^T\mathbf{Z}_2)^{-1}\mathbf{Z}_2^T\mathbf{Z}_1 \\ \mathbf{B}_{21} - \mathbf{B}_{22}(\mathbf{Z}_2^T\mathbf{Z}_2)^{-1}\mathbf{Z}_2^T\mathbf{Z}_{1_1} \end{bmatrix} \mathbf{u}_k = \mathbf{0} \tag{29}$$

both schemes can be used in the case of reduced modal data problems, but it is noted that the mode shape projection algorithm is more efficient computationally. Since the mode shape is expanded once and the expanded mode shape is used in the solution of the problem. In the case of Guyan reduction, the eigenvector must be expanded each time the objective function is evaluated.

3.3. Error in the simulation modal data

Data that are obtained experimentally have always some error. This error, which cannot be avoided, depends on the accuracy of the measuring devices and the experience of the person who conducts the experimental work. Experience has shown that the error in experimental work follows the normal distribution with certain mean and standard deviation. One type of error distribution that is well known in fault detection is the white noise. This type of error, which follows the normal distribution, has zero mean and a standard deviation of unity.

One of the methods for error simulation (Abdalla et al., 2000) that is commonly used in fault detection with maximum percentage error E is given by

$$U_E = U + \frac{N}{100}EU \tag{30}$$

where N is a random number that follows the normal distribution, U_E is the mode shape that has an error level E and U is the error free mode shape. It is noted that in this formula the error is a function of the mode

shape itself. Even though this form is used in fault detection, it is not accurate in simulating errors in measurements, sense the error increases as the modal value U increases, but actually if a physical quantity is measured using a certain device with an accuracy Δ the error is independent of the measured value.

Another formula for error simulation that is commonly used in modeling random error in signal processing and communications, is obtained by adding a random value that is independent of the mode shape itself, this form is given by

$$U_E = U + N\Delta \tag{31}$$

where N is a random number that follows the normal distribution and Δ is a constant that represents the accuracy of the measuring system. The value of Δ can be represented as a certain percentage of the greatest absolute value of the measured modal displacement. Therefore, the noise can be simulated by

$$U_E = U + \frac{E}{100} N U_{\max} \tag{32}$$

this formula is more realistic in simulating experimental error than that formula that is presented in Eq. (30).

4. Numerical examples

In this section, three examples for the application of the crack parameter estimation problem for different structures are presented. These examples are a beam with two cracks, a three-dimensional truss with two cracked elements and a two-dimensional frame with one cracked element.

Since no experimental data is available a simulated experimental data is obtained by solving the corresponding eigenvalue problem of the cracked structure. The error in the simulation modal data is emulated by a white noise given by Eq. (32). When reduced modal data is involved the mode shape projection algorithm is used in expanding the mode shapes.

The factors that are expected to affect the crack parameter estimation results are the error level, the number of modes used and the use of reduced modal data. The effect of these factors will be demonstrated through out the presented examples.

4.1. A cantilever beam with two cracks

Fig. 1 shows a rectangle cross-section cantilever beam with two uniform depth cracks. The beam is made of steel with modulus of elasticity $E = 207$ GPa and mass density $= 7795$ kg/m^3. The cracks are located at 0.25 and 0.65 m from the fixed end and have crack depth ratios of 0.35 and 0.25, respectively. This beam is divided into 10 finite elements each 0.1 m long.

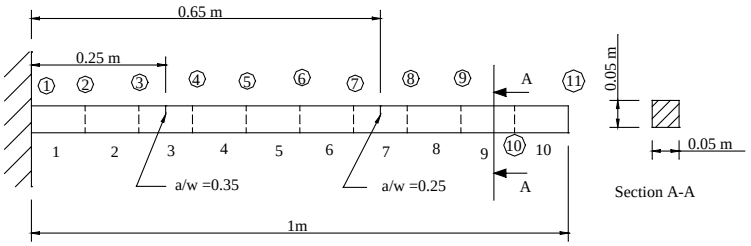

Fig. 1. Rectangle cross-section cantilever beam with two cracks.

The crack compliance for this crack is given by (Shpli and Dado, submitted for publication):

$$c = \frac{6w}{EI}\left(1.98\left(\frac{a}{w}\right)^2 - 3.277\left(\frac{a}{w}\right)^3 + 14.251\left(\frac{a}{w}\right)^4 - 31.08\left(\frac{a}{w}\right)^5 + 62.79\left(\frac{a}{w}\right)^6 - 102.171\left(\frac{a}{w}\right)^7 + 146.404\left(\frac{a}{w}\right)^8 - 127.69\left(\frac{a}{w}\right)^9 + 61.504\left(\frac{a}{w}\right)^{10}\right) \quad (33)$$

where w is the beam cross-section height, a is the crack depth, I is the second moment of area of the beam cross-section and E the modulus of elasticity of the beam material.

Fig. 2 shows the estimated crack depth ratio for the cantilever beam with two cracks using the first five complete mode shapes with white nose that have 0.0%, 3.0% and 7.0% error levels. The figure indicates that the error in the estimated results increased as the error level is increased. Cracks with small depth ratios are indicated in the healthy elements due to the error in the modal data. The estimated depth ratios for these cracks depend on the error level. It is clear that small cracks may be lost and the crack with the smallest depth ratio that can be detected accurately depends on the level of error in the modal data.

Table 1 shows the estimated crack location for this case which indicates that the cracks location for the actual cracks are recovered accurately.

Fig. 3 shows the estimated crack depth ratio for the same beam using complete modal data with white noise that has 3.0% error level and using the first three, five and seven mode shapes. The results indicate that the error in the estimated crack depth ratio decreases as the number of modes increases.

Fig. 4 shows the estimated crack depth ratio for the same cantilever beam using error free modal data. The results represented in this figure are obtained using the first three and five mode shapes for complete and reduced modal data. In the cases of reduced modal data only the translation displacements are used. This figure indicates that both the crack depth ratio and the crack location are recovered accurately regardless of the number of modes and wither complete or reduced modal data is used.

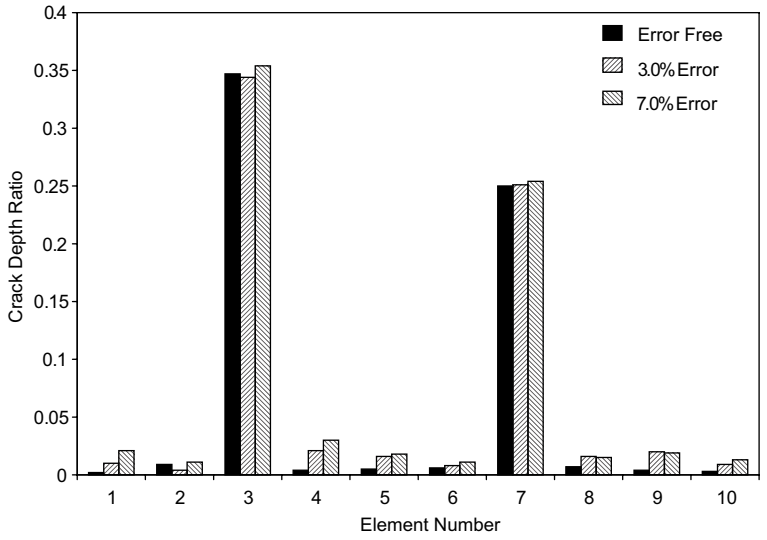

Fig. 2. The estimated crack depth ratio for a cantilever beam with two cracks using the first five complete mode shapes and white noise with different error levels.

Table 1
Estimated crack location for a cantilever beam with two cracks using the first five complete mode shapes and different noise levels with zero mean

No.	Crack location in element local coordinates (m)		
	0.0% noise	3.0% noise	7.0% noise
1	0.057	0.100	0.042
2	0.050	0.100	0.000
3	0.050	0.050	0.050
4	0.037	0.050	0.052
5	0.010	0.025	0.045
6	0.083	0.100	0.100
7	0.050	0.050	0.050
8	0.093	0.080	0.043
9	0.010	0.047	0.100
10	0.060	0.038	0.101

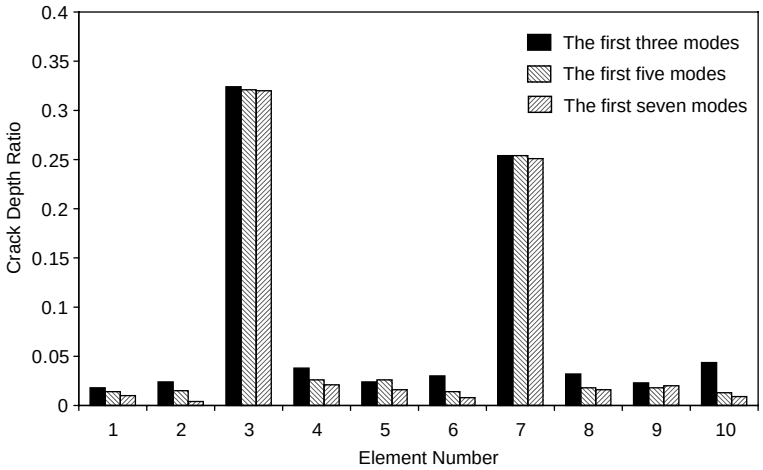

Fig. 3. The estimated crack depth ratio for a cantilever beam with two cracks using complete modal data with white noise that has 3.0% error level and different numbers of mode shapes.

Fig. 5 shows the effect of the mean of the error distribution on the estimated crank depth ratio for the cantilever beam shown in Fig. 1. The results shown in Fig. 5 were obtained using the first five mode shaper with 2.0% error level. The reduced modal data used in the crack parameter estimation are the transverse displacements at nodes two to eleven. It is noted that as the mean of the error distribution increases the error in the estimated results increases. Even though the actual defects can be identified.

4.2. Three-dimensional truss with two cracks

Fig. 6 shows a three-dimensional truss consisting of 18 elements that are connected between nine nodes. Each element has a rectangle cross-section with a cross-section modulus $EA = 517.5$ M N and material density $\rho = 7795$ kg/m^3. The truss has two cracked elements that are element 3 with a crack depth ratio of 0.40 and element 13 with 0.28 crack depth ratio.

The axial compliance for a uniform crack of depth a in rectangle cross-section element is (Shpli and Dado, submitted for publication):

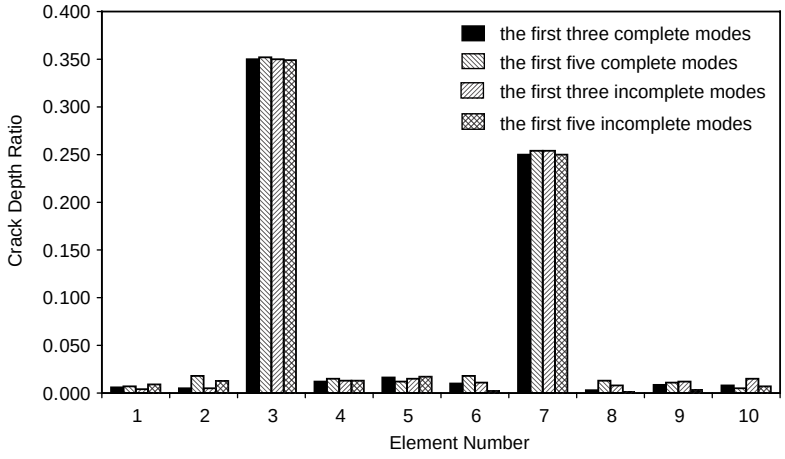

Fig. 4. The estimated crack depth ratio for a cantilever beam with two cracks using error-free reduced modal data with different numbers of mode shapes.

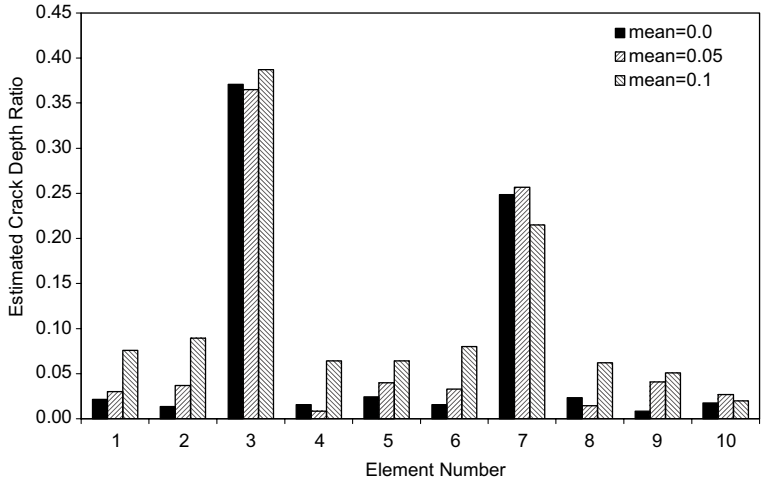

Fig. 5. The estimated crack depth ratio for a cantilever beam with two cracks using the first five reduced mode shapes with 2.0% error level and different values for the mean of the error distribution.

$$c = \frac{2w}{AE}\left(3.9601\left(\frac{a}{w}\right)^2 - 1.08786\left(\frac{a}{w}\right)^3 + 37.2970\left(\frac{a}{w}\right)^4 - 67.3973\left(\frac{a}{w}\right)^5 + 199.848\left(\frac{a}{w}\right)^6 - 424.037\left(\frac{a}{w}\right)^7 + 883.025\left(\frac{a}{w}\right)^8 - 938.075\left(\frac{a}{w}\right)^9 + 601.704\left(\frac{a}{w}\right)^{10}\right) \tag{34}$$

where w is the height of the element cross-section, a is the crack depth, A is the element cross-section area and E is the modulus of elasticity of the element material.

Fig. 7 shows the estimated crack depth ratios for the three dimensional truss using the first five complete mode shapes with white noise that have 0.0%, 3.0% and 7.0% error level. The figure indicates that the error

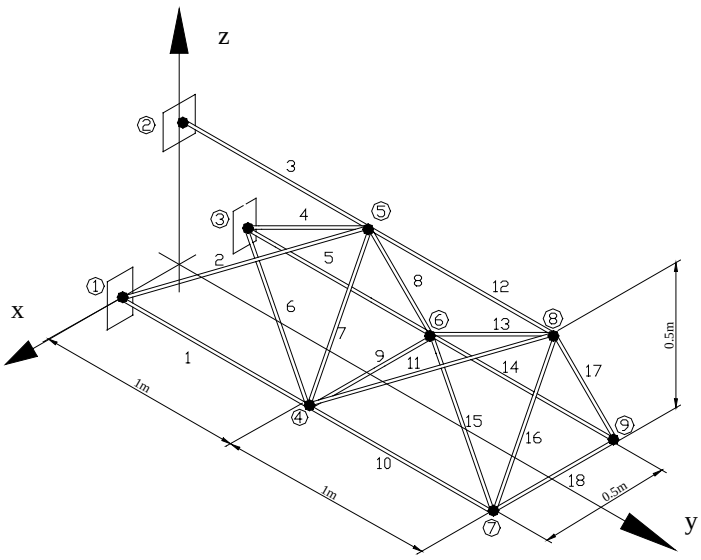

Fig. 6. Three-dimensional truss with two cracked elements.

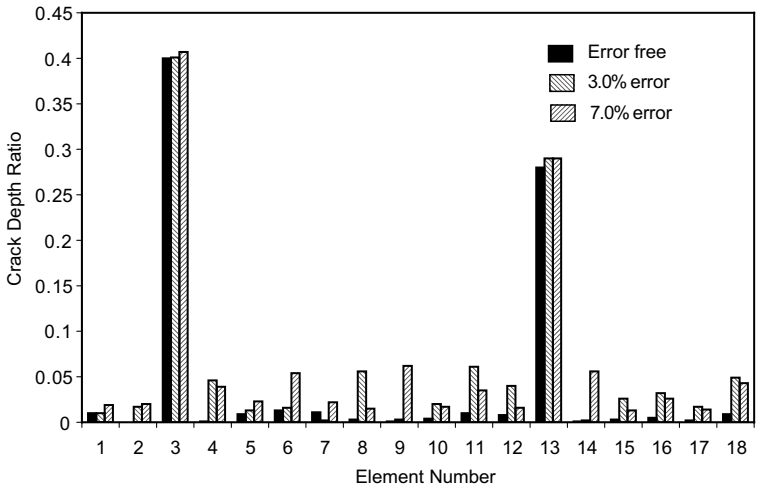

Fig. 7. The estimated crack depth ratio for a three-dimensional truss with two cracks using the first five complete mode shapes and white noise with deferent levels of error.

in the estimated crack depth ratio increases by increasing the error level, but still the actual cracks are clearly indicated.

Fig. 8 shows the estimated crack depth ratios for the same truss using the first five mode shapes with white noise that has 3.0% error level. In this figure the results for complete modal data along with two cases of incomplete modal data are shown. The degrees of freedom encountered in these two cases are shown in Table 2. It is obvious that using reduced modal data will increase the error in the estimated crack parameters. As the number of measured degrees of freedom used in the crack parameter estimation problem decreases the error in the estimated crack depth ratio and crack location increases.

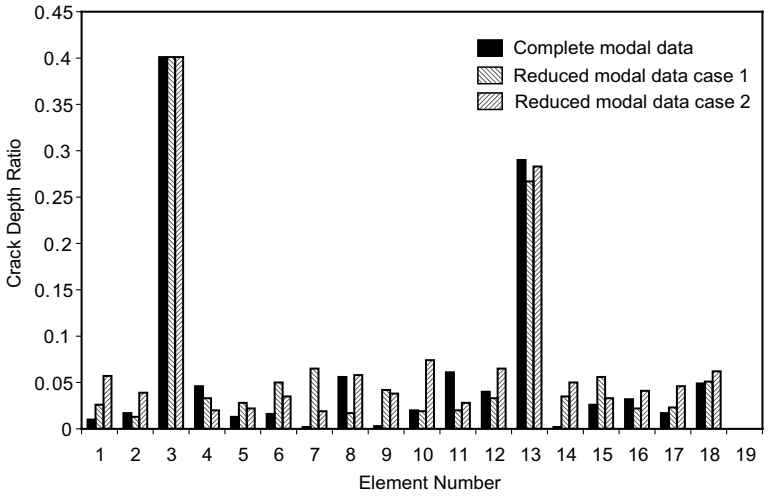

Fig. 8. The estimated crack depth ratio for three-dimension truss using the first five modes with white noise that has 3.0% error and different cases of reduced modal data.

Table 2
Measured degrees of freedom in the cases of reduced modal data for a three-dimensional truss with two cracks

Case no.	x	y	z
Case 1	9,8,7	9,7,5	8,7,5
Case 2	9,5	8,6	7,4

4.3. Two-dimensional frame with one crack

Fig. 9 shows a two-dimensional frame structure that consists of 12 elements connected between 8 joints. Each element has a rectangle cross-section with modulus of elasticity $E = 207$ GPa and density $\rho = 7795$ kg/m^3. The frame has one cracked element that is element 10. The crack is located at 0.35 m for joint 5 and has a crack depth ratio of 0.28.

The crack compliance elements (c_{11}, $c_{33}c_{13}$ and c_{31}) for a uniform depth crack in a rectangle cross-section element can be derived using Eq. (5) and the appropriate expressions for the stress intensity factor. The crack compliance elements c_{11} and c_{33} are given by Eqs. (34) and (33) respectively. The coupling compliance elements c_{13} and c_{31} are equal and given by (Shpli and Dado, submitted for publication):

$$\begin{aligned} c_{13} &= c_{31} \\ &= \frac{6}{EA}\left(1.98\left(\frac{a}{w}\right)^2 - 1.910\left(\frac{a}{w}\right)^3 + 15.919\left(\frac{a}{w}\right)^4 - 34.823\left(\frac{a}{w}\right)^5 + 83.282\left(\frac{a}{w}\right)^6 \right. \\ &\quad \left. - 152.564\left(\frac{a}{w}\right)^7 + 255.078\left(\frac{a}{w}\right)^8 - 243.972\left(\frac{a}{w}\right)^9 + 132.878\left(\frac{a}{w}\right)^{10}\right) \end{aligned} \tag{35}$$

where w is the height of the element cross-section, a is the crack depth, A is the element cross-section area and E is the modulus of elasticity of the element material.

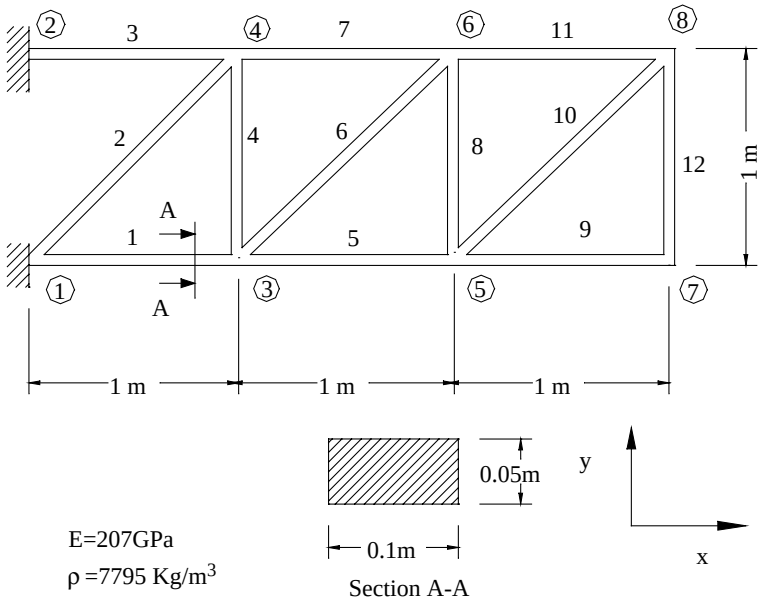

Fig. 9. Two-dimensional frame structure.

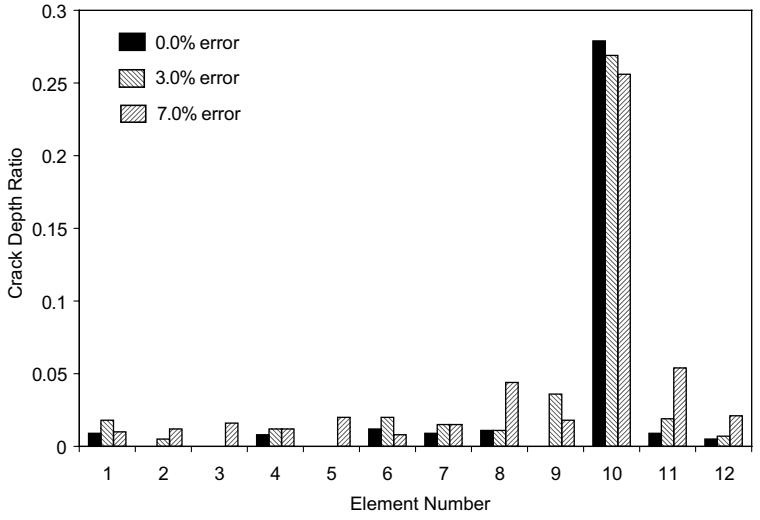

Fig. 10. The estimated crack depth ratio for a two-dimensional frame with one cracked element using the first five complete mode shapes with white noise that has different error levels.

Fig. 10 shows the estimated crack depth ratio for this frame structure using the first five complete mode shapes with white noise that have 0.0%, 3.0% and 7.0% error level. The results show that the estimated crack depth ratio for the true cracks are estimated accurately. The error in the estimated crack depth ratio depends on the level of error in the modal data.

5. Conclusions

This study showed that the cracked finite element models are efficient in estimating the crack depth ratio and location in complex structures. The results are affected by the noise level, the number of modes used and the reduced modal data. Cracks with small depth ratio are extremely affected by these factors and may be completely lost while cracks with high depth ratio are quantified accurately. It is also noted that using error free modal data will result in accurate estimation of the crack depth ratio regardless of the number of modes and wither complete or incomplete modal data is used.

Appendix A. Finite element models for cracked simple structural elements

Finite element models for cracked structural elements (Shpli and Dado, submitted for publication).

A.1. Finite element model for cracked axially loaded element

$$k_{\mathrm{d}} = \frac{EA}{l + EAc}\begin{bmatrix} 1 & -1 \\ -1 & 1 \end{bmatrix} \tag{A.1}$$

where E the modulus of elasticity, A the cross-section area, l the length of the element and c is the crack compliance.

A.2. Finite element model for cracked beam element

$$k_{\mathrm{d}} = \frac{6EI}{\Delta}\begin{bmatrix} 6(l+cEI) & 3(l^2+2xcEI) & -6(l+cEI) & 3(l^2+2(l-x)cEI) \\ 3(l^2+2xcEI) & 2(l^3+3x^2cEI) & -3(l^2+2xcEI) & (l^3+6x(l-x)cEI) \\ -6(l+cEI) & -3(l^2+2xcEI) & 6(l+cEI) & -3(l^2+2(l-x)cEI) \\ 3(l^2+2(l-x)cEI) & (l^3+6x(l-x)cEI) & -3(l^2+2(l-x)cEI) & 2(l^3+3(l-x)^2cEI) \end{bmatrix} \tag{A.2}$$

$$\Delta = 9(l^2+2xcEI)(l^2+2(l-x)cEI) - 6(l+cEI)(l^3+2x(l-x)cEI)$$

where E is the modulus of elasticity of the element material, I the second moment of area of the element cross-section, l the length of the element, x is the location of the crack in element local coordinates and c is the crack compliance.

A.3. Finite element model for a cracked two-dimensional frame element

$$k = \frac{1}{\Delta}\begin{bmatrix} k_{11} & k_{12} \\ k_{21} & k_{22} \end{bmatrix} \tag{A.3}$$

$$\Delta = -\frac{l^2}{3IE}\left[(l^2 - 3x(l-x))\left(c_{11}c_{33} - c_{13}c_{31} + \frac{c_{33}l}{AE}\right) + \frac{l^3(l + c_{11}AE)}{4AIE^2}\right]$$

where E is the modulus of elasticity of the element material, A is the element cross-section area, I the second moment of area of the element cross-section, l the length of the element, x is the location of the crack in

element local coordinate, c_{11} the crack compliance in axial loading mode, c_{33} the crack compliance in bending mode of loading, c_{13} the crack axial-bending coupling compliance, c_{31} is the crack bending-axial coupling compliance and kij are 3×3 sub matrices given by

$$k_{11}=\begin{bmatrix} \dfrac{-lc_{33}(l^2-3x(l-x))}{3EI}-\dfrac{l^4}{12I^2E^2} & \dfrac{-c_{13}l(2x-l)}{2EI} & \dfrac{-c_{13}l^2(3x-2l)}{6EI} \\ \dfrac{-c_{31}l(2x-l)}{2EI} & \dfrac{-c_{33}l}{EA}-(c_{11}c_{33}-c_{13}c_{31}) & \dfrac{-c_{33}lx}{AE}-x(c_{11}c_{33}-c_{13}c_{31}) \\ & -\dfrac{l(l+c_{11}EA)}{2AIE^2} & -\dfrac{l^2(l+c_{11}EA)}{2AIE^2} \\ \dfrac{-c_{31}l^2(3x-2l)}{6EI} & \dfrac{-c_{33}lx}{AE}-x(c_{11}c_{33}-c_{13}c_{31}) & \dfrac{-c_{33}lx^2}{AE}-x^2(c_{11}c_{33}-c_{13}c_{31}) \\ & -\dfrac{l^2(l+c_{11}EA)}{2AIE^2} & -\dfrac{l^3(l+c_{11}EA)}{2AIE^2} \end{bmatrix}$$

$$k_{12}=\begin{bmatrix} \dfrac{c_{33}l(l^2-3x(l-x))}{3IE}+\dfrac{l^4}{12EI^2} & \dfrac{c_{31}l(2x-l)}{2EI} & -\dfrac{c_{31}l^2(2x-l)}{6EI} \\ \dfrac{c_{31}l(2x-l)}{2EI} & \dfrac{c_{33}l}{EA}+(c_{11}c_{33}-c_{13}c_{31}) & -\dfrac{c_{33}l(l-x)}{EA}-(l-x)(c_{11}c_{33}-c_{13}c_{31}) \\ & +\dfrac{l(l+c_{11}EA)}{AIE^2} & +\dfrac{l^2(l+c_{11}EA)}{2AIE^2} \\ \dfrac{c_{31}l^2(2x-l)}{6EI} & \dfrac{c_{33}lx}{EA}-x(c_{11}c_{33}-c_{13}c_{31}) & -\dfrac{c_{33}xl(l-x)}{EA}-x(l-x)(c_{11}c_{33}-c_{13}c_{31}) \\ & +\dfrac{l^2(l+c_{11}EA)}{2AIE^2} & +\dfrac{l^3(l+c_{11}EA)^2}{6AIE} \end{bmatrix}$$

$$k_{21}=\begin{bmatrix} \dfrac{c_{33}l(l^2-3x(l-x))}{3IE}+\dfrac{l^4}{12EI^2} & \dfrac{c_{31}l(2x-l)}{2EI} & -\dfrac{c_{31}l^2(2x-l)}{6EI} \\ \dfrac{c_{31}l(2x-l)}{2EI} & \dfrac{c_{33}l}{EA}+(c_{11}c_{33}-c_{13}c_{31}) & -\dfrac{c_{33}l(l-x)}{EA}-(l-x)(c_{11}c_{33}-c_{13}c_{31}) \\ & +\dfrac{l(l+c_{11}EA)}{AIE^2} & +\dfrac{l^2(l+c_{11}EA)}{2AIE^2} \\ \dfrac{c_{31}l^2(2x-l)}{6EI} & \dfrac{c_{33}lx}{EA}-x(c_{11}c_{33}-c_{13}c_{31}) & -\dfrac{c_{33}xl(l-x)}{EA}-x(l-x)(c_{11}c_{33}-c_{13}c_{31}) \\ & +\dfrac{l^2(l+c_{11}EA)}{6AIE^2} & +\dfrac{l^3(l+c_{11}EA)}{2AIE^2} \end{bmatrix}$$

$$k_{22}=\begin{bmatrix} \dfrac{-c_{33}(l^2-3x(l-x))}{3EA} & -\dfrac{c_{13}l(2x-l)}{2EI} & \dfrac{c_{13}l^2(3x-l)}{6EI} \\ -\dfrac{l^4}{12I^2E^2} & & \\ -\dfrac{c_{13}l(2x-l)}{2EI} & -\dfrac{c_{33}l}{EA}-(c_{11}c_{33}-c_{13}c_{31}) & \dfrac{c_{33}l(l-x)}{EA}+(l-x)(c_{11}c_{33}-c_{13}c_{31}) \\ & -\dfrac{l(l+c_{11}EA)}{AIE^2} & +\dfrac{l^2(l+c_{11}EA)}{2AIE^2} \\ \dfrac{c_{13}l^2(3x-l)}{6EI} & \dfrac{c_{33}l(l-x)}{EA}+(l-x)(c_{11}c_{33}-c_{13}c_{31}) & -\dfrac{c_{33}l(l-x)^2}{EA}-x(l-x)(c_{11}c_{33}-c_{13}c_{31}) \\ & +\dfrac{l^2(l+c_{11}EA)}{2AIE^2} & -\dfrac{l^3(l+c_{11}EA)}{3AIE^2} \end{bmatrix}$$

References

Abdalla, M.O., Grigoriadlis, K.M., Zimmerman, D.C., 2000. Structural damage detection using linear matrix inequality methods. Journal of Vibration and Acoustics 122, 440–455.

Dado, M.H., 1997. Comprehensive crack identification algorithm for beams under different end conditions. Applied Acoustics 51 (4), 381–398.A.

Dado, M.H.F., Abuzid, O. Coupled transverse and axial vibration behavior of cracked beam with end mass and rotary inertia. Journal of Sound and Vibration, in press.

Dimarogonas, A.D., Stephen, A.P., 1983. Analytical Methods in Rotor Dynamics. Applied Science Publishers Ltd., New York.

Fox, C.H.J., 1992. The location of defects in structures: a comparison of the use of natural frequency and mode shape data. In: Proc. of the 10th International Modal Analysis Conference, pp. 522–528.

Friswell, M.I., Penny, J.E.T., Wilson, S.A.L., 1994. Using vibration data and statistical measures to locate damage in structures. Modal Analysis: The International Journal of Analytical and Experimental Modal Analysis 9 (4), 239–254.

Friswell, M.I., Penny, J.E.T., Garvey, S.D., 1997. Parameter subset selection in damage location. Inverse Problems in Engineering 5 (3), 189–215.

Friswell, M.I., Garvey, S.D., Penny, J.E.T., 1998. The convergence of the iteration IRS method. Journal of Sound and Vibration 211 (1), 123–132.

Friswell, M.I., Penny, J.E.T., Garvy, S.D., 1998. A combined genetic and eigensensitivity algorithm for the location of damage in structures. Computers and Structures 69, 547–556.

Kaouk, M., Zimmerman, D.C., 1994. Structural damage assessment using a generalized minimum rank perturbation theory. AIAA Journal 32 (4), 836–842.

Kim, H.M., Bartkowicz, T.J., 1993. Damage detection and health monitoring of large space structures. Journal of Sound and Vibration 27 (6), 12–17.

Lin, C.S., 1990. Location of modeling errors using modal test data. AIAA Journal 28, 1650–1654.

Linder, D.K., Goff, R., 1993. Damage detection, location and estimation for space trussed. SPIE Smart Structures And Intelligent Systems 1917, 1028–1039.

Mays, R.L., 1992. Error localization using mode shapes: an application to a two link Robot arm. In: Proc. 10th Internal Modal Analysis Conference, pp. 889–891.

Mottershead, J.E., Friswell, M.I., 1993. Model update in structural dynamics: a survey. Journal of Sound and Vibration 157 (2), 347–375.

Pandy, A.K., Biswas, M., Samman, M.M., 1991. Damage detection from changes in curvature mode shapes. Journal of Sound and Vibration 145 (2), 321–332.

Park, Y.S., Park, H.S., Lee, S.S., 1988. Weighted-error-matrix application to detect stiffness damage-characteristic measurement. Modal Analysis: The International Journal of Analytical and Experimental Modal Analysis 3 (3), 101–107.

Ruotolo, R., Surace, C., 1997. Damage assessment of multiple cracked beams: numerical results and experimental validation. Journal of Sound and Vibration 206 (4), 567–588.

Scott, W.D., Caarles, R.M., Farrar, B., Shevitz, D.W., 1996. Damage identification and health monitoring of structures from changes in their vibration characteristics: a literature review. Tech. Rep., Los Alamos, New Mexico.

Shpli, O.A., Dado, M.H.F., 2002. Natural frequencies estimation of cracked structures using a finite element model. Journal of Sound and Vibration, submitted for publication.

Simth, S.W., 1992. Iterative use of direct matrix update: connectivity and convergence. In: Proc. 33rd AIAA Structures, Structural Dynamics And Materials Conference, pp. 1797–1806.

West, W.M., 1984. Illustration of the use of modal assurance criterion to detect structural changes in an orbiter test specimen. In: Proc. Air Force Conference On Aircraft Structural Integrity, pp. 1–6.